Available online at www.sciencedirect.com
SCIENCE DIRECT®
Physics and Chemistry of the Earth 31 (2006) 273–280
PHYSICS and CHEMISTRY of the EARTH
www.elsevier.com/locate/pce

ULF geomagnetic perturbations due to seismic noise produced by rock fracture and crack formation treated as a stochastic process

V.V. Surkov [a,*], M. Hayakawa [b]

[a] *Moscow Engineering Physics Institute, 31 Kashirskaya road, Moscow 115409, Russia*
[b] *The University of Electro-Communications, Chofu, Tokyo 182-8585, Japan*

Accepted 6 February 2006
Available online 19 May 2006

Abstract

A mechanism of ULF geomagnetic field perturbations caused by rock fracture and tectonic activity is studied. It is assumed that the rock fracture is accompanied by crack-generated seismic emission due to cracks pile up at underground cracked zones. Temporal series of seismic impulses due to the crack growth is supposed to be a stationary random process, which obeys Poisson distribution. The seismic emission of the cracks results in excitation of electric current due to motion of the conductive ground in the geomagnetic field, that is so-called diamagnetic effect in moving conductors immersed in the external magnetic field. The electric currents build up as a result of the random displacements in the conductive rock, which in turn leads to the random perturbations of the geomagnetic field. Acoustic wave field derivable from the crack seismic moment is used in order to obtain the electromagnetic variations due to growth of single crack. Averaging of these variations over random crack plane orientation and over crack sizes gives an assessment of mean level of the electromagnetic noise produced by the evolution of the crack ensemble. This assessment is consistent in magnitude with the ULF electromagnetic variations recorded prior to and after some strong earthquakes.

Keywords: Rock fracture; Acoustic emission; ULF geomagnetic perturbation; Random process; Earthquake prediction; Ground conductivity; Seismic moment; Magnetic moment

1. Introduction

A special credit has been paid in the past to the study of telluric potential variations (Varotsos and Alexopoulos, 1984a,b) and of ULF electromagnetic noises occasionally observed before and after strong crust earthquakes (Fraser-Smith et al., 1990; Kopytenko et al., 1990; Hayakawa et al., 1996, 2000; Hayakawa and Hattori, 2004). The increases in the ULF noise were happened in the background of low magnetospheric activity and due to that events can be considered as possible precursors of impending earthquakes. To explain this phenomenon, a model based on electrokinetic effect arising from underground fluid migration under the influence of tectonic stress has been developed (Bernard, 1992). Fenoglio et al. (1995) have suggested that the rock contains sealed underground compartments with high pore pressure that may be triggered by weak seismic events, which in turn results in fracture of the compartments and fluid filtration followed by the electrokinetic effect. Surkov et al. (2002) and Surkov and Tanaka (2005) have developed a theory of the electrokinetic phenomena in a water-porous medium with a fractal structure above percolation threshold. The relevance of the stress generated percolation processes to the ground based observations is stressed.

It is noteworthy that the intrinsic conductivity of the rock due to mobile point and linear defects of atomic lattice could have an important role to play in seismoelectric signals observed prior to crust earthquakes (Varotsos and Alexopoulos, 1986; Slifkin, 1993). Based on the

* Corresponding author. Tel.: +7 095 3239835; fax: +7 095 3007516.
E-mail addresses: surkov@redline.ru (V.V. Surkov), hayakawa@whistler.ee.uec.ac.jp (M. Hayakawa).

1474-7065/$ - see front matter
doi:10.1016/j.pce.2006.02.019

time-resolved impact experiments, Freund (2002) has suggested that the rock conductivity at higher depth is mainly due to the clouds of highly mobile positive hole charge carriers, i.e. defect electrons in the O 2p-dominated valence band minerals. In a model proposed by Molchanov and Hayakawa (1995, 1998), the ULF signals result from electric charges on the walls of micro-cracks situated in the rock near the fault zone. These charges form a fluctuation mosaic of electric dipoles with random orientations. Due to that the signals arise from the charge relaxation are incoherent, which results in drastic decrease of the net electromagnetic signal.

In the present study we develop other theoretical model proposed early (Surkov, 1997, 1999, 2000; Surkov et al., 2003) in order to explain the underlying mechanisms of such an effect. In this study we focus alone on geomagnetic perturbations arisen from rock fracture and energization of crack formation in the rock surrounding the fault zone. Acoustic emission of the cracks results in excitation of electric current due to motion of the conductive ground in the geomagnetic field, that is so-called diamagnetic effect in moving conductors immersed in the external magnetic field. If only tension cracks are considered, as the early modelers did, the geomagnetic perturbations arise in such a way that an effective magnetic moment of the electric currents must be pointed oppositely to the vector of geomagnetic induction. The magnetic moments of all the cracks are thus co-directed independently of the crack plane orientation that results in effective coherent amplification of the ULF geomagnetic perturbations. This model has been extended for the shear cracks (Surkov, 2000; Molchanov et al., 2002), but in this case a certain order in the crack orientation is required in order to produce the coherent effect.

The ULF electromagnetic field propagates in a conductor due to a mechanism similar to diffusion so that the strong dispersion and dissipation of signals take place. The diffusion front of the electromagnetic signal, which propagates ahead of acoustic wave, is referred to as the class of electromagnetic precursor of acoustic wave (Surkov, 2000). This initial smooth part of the electromagnetic signal increases gradually until the moment of acoustic wave arrival at the observation point. It is worth mentioning that at far distance the electromagnetic precursor has the same shape and polarization for all the cracks, while the next stage of the signal, which associates with the acoustic wave arrival, consists of co-seismic oscillations, whose frequency and phase depend on inclination of the geomagnetic field, the crack size and the crack plane orientation. In an early study of the crack-generated geomagnetic perturbations, Surkov et al. (2003) took into account only the initial part of the signals, that is the coherent part, in order to avoid some mathematical complexities.

In this study we develop a more accurate model, which allows for an accidental character in the moments of the crack growth and formation. When calculating the net electromagnetic signal produced by all the cracks, we take into consideration both coherent and incoherent/co-seismic parts of the signals. Since in the model the acoustic emission plays the role of the source of the electromagnetic perturbations, the attenuation of the acoustic waves is of special interest in the present paper. In addition, we take into account a random crack orientation and distribution of the crack sizes.

2. Model and basic equations

Rock deformation due to tectonic activity is accompanied by formation of cracked zones at higher depth and by fall off of the rock strength inside this zones (Scholz, 1990). As we shall see, the rock fracture gives rise to both seismic and electromagnetic noises, which can be detected on the ground surface. The cracked zone is supposed to be located no more than several kilometers from the ground surface; otherwise the rock conductivity will result in a strong damping of the electromagnetic noise. Moreover, suppose that the distance from the cracked zone to the ground-recording station is much greater than the typical crack size. The rock fracture inside the cracked zone results in the crack growth and formation of the fresh crack followed by radiation of acoustic waves. Magnitude of acoustic impulse radiated by a single crack depends on both the crack size and orientation of the crack plane with respect to a sensor. The sequence of acoustic impulses due to the crack growth is supposed to be a stationary random process with the probability for the appearance of impulse obeying Poisson distribution. The conductive ground motion due to acoustic impulses gives rise to generation of the electric current which in turn results in formation of the geomagnetic perturbations. Thus, the geomagnetic perturbations resulted from the acoustic emission of the crack form a random process as well. The net geomagnetic perturbation, $\delta\mathbf{B}_t(\mathbf{r},t)$, is the sum of random impulses

$$\delta\mathbf{B}_t(\mathbf{r},t) = \sum_{k=1}^{n} \delta\mathbf{B}_k(\mathbf{r}, t - t_k, \mathbf{n}_k, l_k), \tag{1}$$

where the unit vector, $\mathbf{n}_k$, normal to the crack plane defines a random orientation of the crack. Likewise, the crack number, n, the moment of radiation onset, t_k, and the crack's size, l_k, are random values. Suppose that all these random values, t_k, $\mathbf{n}_k$ and l_k, are statistically independent of each other and their probability distributions are independent of the impulse number n. Actually there may be a certain degree of correlation between the crack ensemble parameters. The Hurst analysis of the electric signals that precede rupture are in favor of this fact (Varotsos et al., 2002, 2003). At the moment we have not enough information on the crack formation in rocks deep in the crust in order to construct a reasonable approximation to the correlation functions.

Let $\dot{N}(l)$ be the number of crack arising per unit of time with a length greater than l occurring in a specified area.

Since the stationary Poisson process is considered, the averaging of Eq. (1) gives (Rytov, 1966)

$$\overline{\delta \mathbf{B}}_t(\mathbf{r}) = -\int_0^{l_{\max}} \frac{\mathrm{d}\dot{N}(l)}{\mathrm{d}l}\mathbf{b}(\mathbf{r},l)\mathrm{d}l, \tag{2}$$

where

$$\mathbf{b}(\mathbf{r},l) = \int_0^{\infty} \overline{\delta \mathbf{B}_1(\mathbf{r},t,\mathbf{n},l)}\mathrm{d}t, \tag{3}$$

and $\delta\mathbf{B}_1$ is the geomagnetic perturbations due to acoustic emission of a single crack. The bar symbol in Eq. (3) denotes the averaging over the angles defining the random orientation of the vectors $\mathbf{n}_k$ and $l_{\max}$ is the maximal crack size. Below we show that the small cracks make a little contribution to the integral in Eq. (3) due to a strong damping of the acoustic waves radiated by the small cracks. In this picture a minimal crack size in Eq. (3) is unimportant.

The ground is supposed to be a uniform conductor immersed in the constant geomagnetic field $\mathbf{B}_0$. The electromagnetic perturbations, $\delta\mathbf{B}_1$ and $\mathbf{E}_1$, caused by acoustic emission of a single crack satisfy the quasi-stationary Maxwell equation ($\delta B_1 \ll B_0$)

$$\nabla\times\delta\mathbf{B}_1 = \mu_0\sigma\mathbf{E}_1', \quad \mathbf{E}_1' = \mathbf{E}_1 + \mathbf{v}\times\mathbf{B}_0, \tag{4}$$

and

$$\nabla\times\mathbf{E}_1 = -\partial_t\delta\mathbf{B}_1, \tag{5}$$

where the ground conductivity, σ, is a constant, μ_0 is the magnetic constant/permeability of free space, $\mathbf{v}$ is the mass medium velocity, and the symbol ∂_t denotes the partial derivative in time. Here $\mathbf{E}_1$ is the electric field in the reference frame fixed to the earth, while $\mathbf{E}_1'$ stands for the electric field in the moving frame. It should be noted that the term $\mathbf{v}\times\mathbf{B}_0$ in Eq. (4) plays the role of a source of the electromagnetic perturbations. For convenience, we introduce the vectorial potential via $\delta\mathbf{B}_1 = \nabla\times\mathbf{A}_1$ and $\mathbf{E_1} = -\partial_t\,\mathbf{A}_1$, which satisfies the standard gauge for conductive medium (e.g., see Molchanov et al., 2002). Substituting the above equations for $\mathbf{A}_1$ into Eqs. (4) and (5), yields

$$\partial_t\mathbf{A}_1 = D\nabla^2\mathbf{A}_1 + \mathbf{v}\times\mathbf{B}_0, \qquad D = (\mu_0\sigma)^{-1}, \tag{6}$$

where D is the coefficient of magnetic diffusion. In order to obtain the time-integrated perturbation $\mathbf{b}(\mathbf{r},l)$ in Eq. (3) one should integrate Eq. (6) with respect to time from 0 to infinity under the condition that $\mathbf{A}_1(0) = \mathbf{A}_1(\infty) = 0$ and then take the mean value over the crack orientation. Taking into account that the mass medium velocity, $\mathbf{v}(\mathbf{r},t)$, can be expressed through the vector of medium displacement, $\mathbf{u}(\mathbf{r},t)$, via $\mathbf{v} = \partial_t\mathbf{u}$, we obtain

$$D\nabla^2\mathbf{a} + \bar{\mathbf{u}}_s\times\mathbf{B}_0 = 0, \tag{7}$$

where $\mathbf{a}$ is the mean value of $\mathbf{A}_1$, $\mathbf{b} = \nabla\times\mathbf{a}$ and the vector $\bar{\mathbf{u}}_s = \bar{\mathbf{u}}(\mathbf{r},\infty)$ defines the static/residual displacements in the medium. These displacements are assumed to be maximal inside the cracked zone and they should gradually decline in the surrounding rock.

3. Averaging over the crack orientation

In order to study the residual displacements due to formation and evolution of the crack ensemble we first consider a dynamic displacement field due to single crack growth. Acoustic waves generated by the growing crack in a uniform elastic medium are defined by the wave equation

$$\rho\partial_t^2\mathbf{u} = (\lambda+2\mu)\nabla(\nabla\cdot\mathbf{u}) - \mu\nabla\times(\nabla\times\mathbf{u}), \tag{8}$$

where λ and μ are the Lame coefficients and ρ is the rock density. If the distance is much greater than the crack size, the solution of Eq. (8) can be expressed through the so-called seismic moment tensor, $\widehat{\mathbf{M}}$, of the crack. For example, let us consider a tension flat crack lying in the x', y' plane of the local coordinate system fixed to the crack. Let $[u_z(t)] = u_z(t,z'=0+) - u_z(t,z'=0-)$ be a given function, which defines the displacement jump/discontinuity normal to the crack surface and parallel to the z'-axis. In this case only three diagonal components of the seismic moment tensor are non-zero (Aki and Richards, 2002)

$$M_{xx} = M_{yy} = \lambda S[u_z(t)], \qquad M_{zz} = (\lambda+2\mu)S[u_z(t)], \tag{9}$$

where S is the area of the crack surface. The crack growth gives rise to changes in the seismic moment, which in turn results in the radiation of seismic waves. The components of medium displacement, $u_i(\mathbf{r}',t)$, is derivable from the wave equation (8) via the seismic moment in the following way

$$\begin{aligned} u_i = \frac{\gamma_i'}{4\pi\rho r'}\Bigg\{ & \frac{[6f_1(t_1) - f_2(t_1) - 2M_{ii}(t_1)]}{r'C_l^2} \\ & - \frac{[6f_1(t_2) - f_2(t_2) - 3M_{ii}(t_2)]}{r'C_t^2} \\ & + \partial_t\left(\frac{f_1(t_1)}{C_l^3} - \frac{[f_1(t_2) - M_{ii}(t_2)]}{C_t^3}\right) \\ & + \frac{3}{r'^3}\widehat{\mathbf{G}}(5f_1 - f_2 - 2M_{ii})\Bigg\}, \end{aligned} \tag{10}$$

where r' is the distance from the crack, $C_l = [(\lambda+2\mu)/\rho]^{1/2}$ and $C_t = [\mu/\rho]^{1/2}$ are the velocities of longitudinal and transverse acoustic waves, the inferior index $i = x', y', z'$ and

$$f_1 = (\gamma_x'^2 + \gamma_z'^2)M_{xx} + \gamma_z'^2 M_{zz}, \qquad f_2 = 2M_{xx} + M_{zz},$$
$$t_1 = t - \frac{r'}{C_l}, \qquad t_2 = t - \frac{r'}{C_t}. \tag{11}$$

The direction cosines, γ_i', can be written as $\gamma_x' = x'/r'$, $\gamma_y' = y'/r'$ and $\gamma_z' = z'/r'$, and the integral operator $\widehat{\mathbf{G}}$ is defined in the following manner

$$\widehat{\mathbf{G}}M_{ii} = \int_{r'/C_l}^{r'/C_t} \tau M_{ii}(t-\tau)\mathrm{d}\tau, \tag{12}$$

The set of Eqs. (9)–(12) contains both the near- and far-field displacement components. As it follows from the general solution, the crack opening produces both the longitudinal and transverse seismic waves, which propagate with different velocities. The corresponding terms in Eq. (10) depend on t_1 and t_2 accordingly. In the static limit when $t \to \infty$ the time-derivatives $\partial_t M_{ii}$ in Eq. (10) vanish, whereas the terms $\widehat{\mathbf{G}} M_{ii}$ tend to the value

$$\widehat{\mathbf{G}} M_{ii} = \frac{M_{ii(s)} r'^2}{2C_t^2}(1-w), \tag{13}$$

where $w = C_t^2/C_l^2$ and $M_{ii(s)} = M_{ii}(\infty)$ is the static/residual value of the seismic moment of the crack. In what follows we omit the inferior index s in order to simplify the expressions for the residual seismic moment. Combining Eqs. (10), (11) and (13), gives the residual displacement field in the form

$$u_i = \frac{\gamma'_i}{8\pi\rho r'^2 C_t^2}[(3f_1 - f_2)(1-w) + 2wM_{ii}], \tag{14}$$

where the functions f_1, f_2 are also taken in static limit, i.e. at $t \to \infty$.

As we have noted above, the rock fracture due to the crack development is predominantly concentrated inside the cracked zone. In what follows we use the general reference frame, x, y, z, fixed to certain point/"center" of the cracked zone. Since we are interested in the distances large compared to the size of the cracked zone, the spatial crack distribution inside the cracked zone is ignored. This implies that the origin of the general reference frame approximately coincides with the origins of the local reference frames associated with separate cracks. The displacement components of each crack should be transformed from the local reference frame, x', y', z', to the general one. For now, the size and plane crack orientation are considered as random values. Let θ_0 and φ_0 be the Euler angles, which define the random orientation of the unit vector $\mathbf{n}$ normal to the crack plane. In addition, we introduce the spherical coordinates, r, θ, φ of the general reference frame. For convenience, both the general and local reference frames are sketched in Fig. 1(a). The crack plane is shown in Fig. 1(a) with grey ellipse. The displacement field of the separate crack in the spherical coordinates can then be expressed through the displacement components in Eq. (14) in the following way:

$$u_r = \gamma'_x u_{x'} + \gamma'_y u_{y'} + \gamma'_z u_{z'}, \tag{15}$$

$$\begin{aligned} u_\theta = {} & u_{x'}(\cos\theta_0\cos\theta\cos(\varphi-\varphi_0) + \sin\theta_0\sin\theta) \\ & + u_{y'}\cos\theta\sin(\varphi-\varphi_0) \\ & + u_{z'}(\sin\theta_0\cos\theta\cos(\varphi-\varphi_0) - \cos\theta_0\sin\theta), \end{aligned} \tag{16}$$

$$\begin{aligned} u_\varphi = {} & -u_{x'}\cos\theta_0\sin(\varphi-\varphi_0) + u_{y'}\cos(\varphi-\varphi_0) \\ & - u_{z'}\sin\theta_0\sin(\varphi-\varphi_0). \end{aligned} \tag{17}$$

The direction cosines are transformed to the view

$$\gamma'_x = \sin\theta\cos\theta_0\cos(\varphi-\varphi_0) - \cos\theta\sin\theta_0, \tag{18}$$

$$\gamma'_y = \sin\theta\sin(\varphi-\varphi_0), \tag{19}$$

$$\gamma'_z = \sin\theta_0\sin\theta\cos(\varphi-\varphi_0) + \cos\theta_0\cos\theta. \tag{20}$$

Substituting Eq. (14) for u_i and Eqs. (18)–(20) for γ'_i into the set of Eqs. (15)–(17), and rearranging, yields

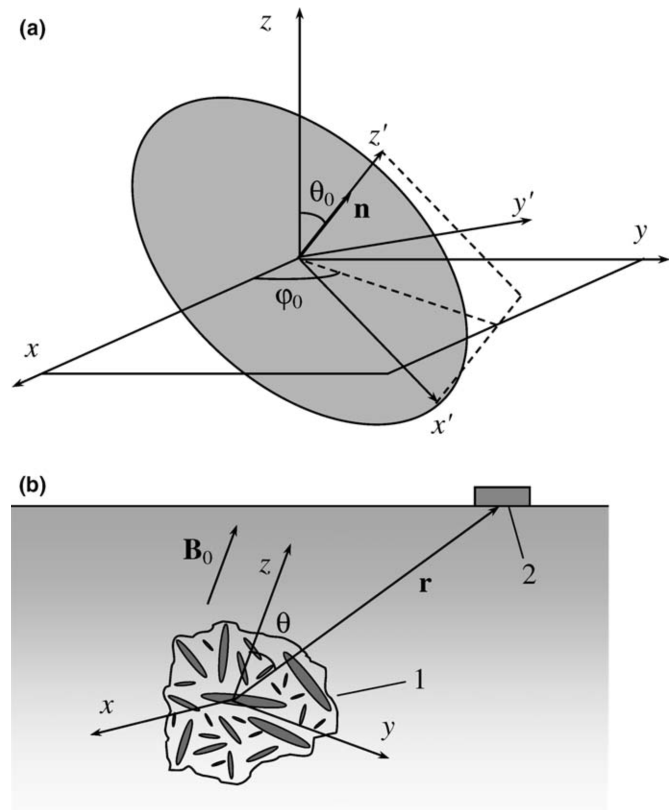

Fig. 1. A schematic plot of a cracked zone model. (a) A general reference frame and a local frame associated with a crack. (b) General scenario. 1 – the cracked zone, 2 – a ground-based recording station.

$$u_r = \frac{1}{8\pi\rho r^2 C_t^2}[(3-w)f_1 - (1-w)f_2], \tag{21}$$

$$\begin{aligned} u_\theta = {} & \frac{\sin 2\theta (M_{zz} - M_{xx})}{8\pi\rho r^2 C_l^2}\Big[\sin^2\theta_0\cos^2(\varphi-\varphi_0) \\ & + \frac{\sin 2\theta_0}{2}\cos 2\theta\cos(\varphi-\varphi_0) - \cos^2\theta_0\Big], \end{aligned} \tag{22}$$

$$u_\varphi = \frac{\sin\theta_0\sin(\varphi-\varphi_0)(M_{xx} - M_{zz})\gamma'_z}{4\pi\rho r^2 C_l^2}. \tag{23}$$

As it is seen from Eqs. (21)–(23), the displacement components depend on the random angles θ_0 and φ_0 as well as on the fixed/deterministic angles θ and φ, which define the direction from the cracked zone to the ground-recording station. Assuming for the moment that there is an equal probability for the crack plane orientation, the probability density distribution does not depend on azimuthal angle φ_0. In such a case the averaging of Eqs. (21)–(23) with respect to φ_0 yields

$$\begin{aligned} \bar{u}_r = {} & \frac{1}{8\pi\rho r^2 C_t^2}\Big\{(M_{xx} - M_{zz})\Big[(3-w)\Big(\frac{\sin^2\theta\sin^2\theta_0}{2} \\ & + \cos^2\theta\cos^2\theta_0\Big) - 1\Big] + w(M_{xx} + M_{zz})\Big\}, \end{aligned} \tag{24}$$

$$\bar{u}_\theta = \frac{\sin 2\theta(M_{zz} - M_{xx})}{8\pi\rho r^2 C_l^2}\left(\frac{\sin^2\theta_0}{2} - \cos^2\theta_0\right), \quad \bar{u}_\varphi = 0. \tag{25}$$

In a similar fashion we can average Eqs. (24) and (25) with respect to the polar angle θ_0. Finally, taking into account that $\overline{\cos^2\theta_0} = 1/3$ and $\overline{\sin^2\theta_0} = 2/3$, we get

$$\bar{u}_r = \frac{u_0}{r^2} \quad \text{and} \quad \bar{u}_\theta = 0, \quad \text{where } u_0 = \frac{(2M_{xx} + M_{zz})}{12\pi\rho C_l^2}. \tag{26}$$

As it follows from Eq. (26), the averaging of the displacement vector gives only the radial component. This means that the mean displacement field is spherically symmetric at far distance from the cracked zone. It is not surprising since the equal probability for the vector **n** orientation is assumed. Conversely, if the probability distribution for the crack plane orientation is non-spherically symmetric, certain declination from Eq. (26) must occur.

For reasons of convenience, all the cracks are considered to have the same disk-shaped form with different radius R. The static displacement jump $[u_z]$ is supposed to be proportional to the crack length $l = 2R$, so that $[u_z] = kl$, where $k = 0.001$–0.01. Combining this expression with Eqs. (9) and (26), yields

$$u_0 = \frac{kl^3}{4\pi}\left(1 - \frac{4w}{3}\right). \tag{27}$$

As we shall see, the attenuation of seismic waves due to dissipation and absorption of the seismic energy in actual rock may greatly affect the magnitude of both the seismic waves and the geomagnetic perturbations. In order to estimate this effect we introduce the acoustic damping factor, $T_a(r,R)$, which depends on the distance and the crack radius. Multiplying $\bar{u}_r$ (Eq. (26)) by this factor, yields

$$\bar{u}_r = \frac{u_0}{r^2} T_a(r,R), \qquad T_a(r,R) = \exp\left(-\frac{r}{L(R)}\right). \tag{28}$$

Here we made use of the exponential form of the damping factor. The characteristic length of the acoustic waves attenuation, L, is estimated as follows (Surkov et al., 2003):

$$L = \alpha R, \qquad \alpha \sim \frac{QC_l}{2\pi C_c}, \tag{29}$$

where C_c is the velocity of crack growth and Q is the quality/energy-factor, which is approximately constant in the frequency range from 10^{-4} to 100 Hz depending on variety of materials (Aki and Richards, 2002). Taking the typical parameters $C_l = 5$ km/s, $C_c = 1.5$ km/s, $Q = 100$ we can estimate the coefficient of proportionality in Eq. (29) as $\alpha \approx 50$. As it follows from Eqs. (28) and (29), the small cracks are of little importance in the sense that their contribution to the net displacement field appears to be exponentially small, while the large cracks make main contribution to the mean displacement and therefore to the crack generated magnetic perturbations.

4. ULF electromagnetic noise generated by random crack ensemble

The equations for the mean displacement field we have thus far obtained implies that all the cracks have a random orientation but the same size/radius. In the analysis that follows, we first seek for the solution of Eq. (7) in the case of cracks with fixed radius, R, and then extend the solution to the case of crack size distribution. Since the mean displacement has been obtained is spherically symmetric, the spherical coordinates r, θ, φ are needed. We shall use a coordinate system in which the z-axis is positive parallel to the vector of geomagnetic field, $\mathbf{B}_0$. For illustrative purposes, the reference frame and the cracked zone are sketched in Fig. 1(b). In the case study all the values are independent of the azimuthal angle φ, and only azimuthal component of **a** is non zero. Eq. (7) is thus reduced to the form

$$\frac{D}{r^2}\left[\partial_r(r^2\partial_r a_\varphi) + \partial_\theta\left\{\frac{\partial_\theta(a_\theta \sin\theta)}{\sin\theta}\right\}\right] = B_0\bar{u}_r(r)\sin\theta, \tag{30}$$

where ∂_r and ∂_θ denote the partial derivatives with respect to r and θ, accordingly, and θ is the polar angle included between the vectors $\mathbf{B}_0$ and $\mathbf{r}$. We seek for the solution of Eq. (30) in the form $a_\varphi = g(r)\sin\theta$. Substituting this function and Eq. (28) for $\bar{u}_r$ into Eq. (30), yields

$$d_r(r^2 d_r g) - 2g = \frac{u_0 B_0}{D}\exp\left(-\frac{r}{L}\right), \tag{31}$$

where $d_r = \mathrm{d}/\mathrm{d}r$. This differential equation (31) has a straightforward analytical solution

$$g(x) = c_1 x + \frac{c_2}{x^2} + \frac{u_0 B_0}{3D}\left[\left(\frac{1}{x^2} + \frac{1}{x} - 1\right)\exp(-x) + xE_1(x)\right], \tag{32}$$

where c_1 and c_2 are arbitrary constants, $x = r/L$ and $E_1(x)$ denotes the exponential integral, that is

$$E_1(x) = \int_x^\infty \frac{\exp(-x')}{x'}\mathrm{d}x'.$$

One makes sure of validity of the solution by direct substitution of Eq. (32) for $g(r)$ into Eq. (31). The sought function **b** can be expressed through $g(x)$ in the following manner

$$\mathbf{b} = \frac{1}{r}[2\hat{\mathbf{r}}g(x)\cos\theta - \hat{\boldsymbol{\theta}}\partial_r\{rg(x)\}\sin\theta]. \tag{33}$$

In order to find c_1 and c_2 these equations should be supplemented by the proper boundary conditions. Since the function **b** in Eq. (33) must go to zero at infinity, we get that $c_1 = 0$. Moreover, **b** must to be limited when $r \to 0$. Eventually, we obtain that

$$g(x) = \frac{u_0 B_0}{3D}\left[\left(\frac{1}{x^2} + \frac{1}{x} - 1\right)\exp(-x) - \frac{1}{x^2} + xE_1(x)\right]. \tag{34}$$

Consider first the case of large distances/small cracks. From the analysis of Eq. (34) it follows that when $r \gg L$ ($x \gg 1$) the function $g(x)$ simplifies to

$$g \approx -\frac{u_0 B_0}{3Dx^2}. \tag{35}$$

Once the maximal crack size satisfies the inequality $l_{\max} \ll r/\alpha$, where α is given by (29), this approach is valid for all the cracks. Substituting of Eq. (35) for g into Eq. (33), yields

$$\mathbf{b} \approx -\frac{u_0 B_0 L^2}{3Dr^3}(2\hat{\mathbf{r}}\cos\theta + \hat{\theta}\sin\theta), \tag{36}$$

where $\hat{\mathbf{r}}$ and $\hat{\boldsymbol{\theta}}$ denote the unit vectors.

For now, we shall be interested in the averaging over the crack size. We suppose that the number of crack arising per unit of time with a length greater than l occurring in a specified area can be estimated from the known empirical law obtained by Gutenberg and Richter (1954) for the number of earthquakes. According to Turcotte (1997)

$$\dot{N}(l) = \frac{\dot{\beta}}{l^{2b}}, \tag{37}$$

where b is the dimensionless empirical constant, whose value varies from region to region but is generally in the range $0.8 < b < 1.2$. The constant $\dot{\beta}$ is a measure of the regional level of seismicity. This value is measured in units of m^{2b}/s. The worldwide data correlate with (37) taking $b = 1.11$ and $\dot{\beta} \approx 2 \times 10^3$ m^{2b}/s. Assuming for the moment that the dependence (37) can be extrapolated down to the crack sizes of about several meters and combining Eq. (37) and Eq. (2), yields

$$\overline{\delta\mathbf{B}_t}(\mathbf{r}) = 2b\dot{\beta}\int_0^{l_{\max}} \frac{\mathbf{b}(\mathbf{r}, l)}{l^{2b+1}}\,\mathrm{d}l. \tag{38}$$

Substituting Eq. (36) for $\mathbf{b}$ into Eq. (38) and performing integration over l, gives the sought value of the mean magnetic perturbations. The result of integration can be written as a field of magnetic dipole

$$\overline{\delta\mathbf{B}_t}(\mathbf{r}) = -\frac{\mu_0}{4\pi}\nabla\frac{(\mathbf{p}_m\cdot\mathbf{r})}{r^3}, \tag{39}$$

where

$$\mathbf{p}_m = -\frac{\sigma\dot{\beta}kb\alpha^2 l_{\max}^{5-2b}}{6(5-2b)}\left(1 - \frac{4w}{3}\right)\mathbf{B}_0.$$

The effective magnetic moment, $\mathbf{p}_m$, is directed in opposition to the unperturbed geomagnetic field $\mathbf{B}_0$. It is not surprising since the conductor motion in external magnetic fields must result in usual diamagnetic effect, which makes for formation of the effective magnetic moment with negative sign (Surkov, 2000). The case treated here corresponds to strong attenuation because the distance, r, from the cracked zone is much greater than the effective damping length $L_{\max} \sim \alpha l_{\max}$ of the seismic waves emitted by the cracks. As it is seen from the solution (39), the average level of the electromagnetic noise in this region decreases as r^{-3}. It follows from our numerical estimation that at such far distances the crack generated electromagnetic noise is practically undetectable and thus this case-study is of little importance.

For short distances of interest here, that is $r \ll \alpha l_{\max} \sim 50 l_{\max}$, the contribution of the small and large cracks to the integral (38) should be estimated separately. As it follows from Eq. (36), which is valid for the small cracks with length $l \ll r/\alpha$, the function $\mathbf{b}(\mathbf{r},l)$ is proportional to l^5 and hence the integrand in Eq. (38) is proportional to $l^{4-2b} \approx l^{1.8}$, where b is the fractal dimension in Eq. (37). In the case of the large cracks when $x \ll 1$, Eq. (34) for g is transformed to

$$g \approx -\frac{u_0 B_0}{2D}. \tag{40}$$

In this picture the attenuation of the seismic waves radiated by large cracks is nearly unimportant. Substituting Eq. (40) for g into Eq. (33), yields

$$\mathbf{b} \approx -\frac{u_0 B_0}{2Dr}(2\hat{\mathbf{r}}\cos\theta - \hat{\boldsymbol{\theta}}\sin\theta). \tag{41}$$

It follows from Eq. (41) that as long as $l \gg r/\alpha$ the function $\mathbf{b}(\mathbf{r},l) \propto l^3$ and therefore the integrand in Eq. (38) is proportional to $l^{2-2b} \approx l^{-0.2}$. The rough estimating of the contributions to the integral (38) due to the small and large cracks gives the ratio $[r/(\alpha l_{\max})]^{3-2b}$. This means that at the distance $r \ll \alpha\, l_{\max}$ the small cracks make a little contribution to the integral sum in Eq. (38) compared to that due to the large cracks. Taking the notice of this fact, substituting Eq. (41) for $\mathbf{b}$ into Eq. (38), yields

$$\overline{\delta\mathbf{B}_t}(\mathbf{r}) = -\frac{\mu_0\sigma B_0\dot{\beta}kbl_{\max}^{3-2b}}{4\pi r(3-2b)}\left(1 - \frac{4w}{3}\right)\left(2\hat{\mathbf{r}}\cos\theta - \hat{\theta}\sin\theta\right). \tag{42}$$

It should be emphasized that Eq. (42) determines, as a matter of fact, only statistical average, which corresponds to the mean level of the crack-induced electromagnetic noise. This rough estimate does not depend on the damping constant α since it holds while the ground-recording station is located not far from the cracked zone.

5. Discussion and conclusions

Our theoretical analysis has shown that the rock fracture must be accompanied by generation of the low-frequency electromagnetic noise. To proceed analytically, we have constructed a suitably idealized model of the cracked zone and of the crack generated geomagnetic perturbations treated as a stochastic process. The predicted level of the ULF electromagnetic noise is found to be proportional to the constant $\dot{\beta}$, which is a measure of the regional level of seismicity. Intense acoustic emission in the frequency band of 0.03–1 kHz along with noticeable ULF magnetic noise have been detected by Gorbatikov et al. (2002) at Matsushiro Observatory, Japan before and after seismic events occurred within distance range of about 150 km. Note that such evidence can serve as an indirect proof/confirmation of the model developed above. According to Scholz (1990), the region of preparing earthquake can occupy the area with size of about several hundred kilometers. Such an area may contain a system of cracked zones with sizes of about 0.1–1 km. Gorbatikov et al. (2002) have assumed that the acoustic emission occasionally observed half a day before the earthquake occurrence may be associated with the energization of the rock fracture inside the cracked zones. The estimation of the acoustic damping factor shows that the source of acoustic emission must be located not far from the ground surface to produce a detectable value of magnetic noise. In other words, the crack generated electromagnetic effect, which may prevail over the background level, can be expected if only the cracked zone is situated not far as 1 km from the ground-recording station.

For the numerical estimation of the magnetic effect caused by rock fracture we take typical parameters of regional seismicity $\dot{\beta} = 2 \times 10^3\ \mathrm{m}^{2b}/\mathrm{s}$ and $b = 1.11$ (Turcotte, 1997) and the following constants $k = 0.01$, $l_{\max} = 1$ km, $\sigma = 10^{-2}$ S/m, $B_0 = 5 \times 10^{-5}$ T, $C_t/C_l = 0.5$ and $\theta = \pi/4$. Suppose also that the magnetometer is situated at the distance $r \approx 1$ km from the cracked zone. Substituting these parameters into Eq. (42), gives the rough assessment of the mean level of the ULF electromagnetic noise $|\overline{\delta \mathbf{B}_t}| \approx 0.3$ pT. It should be noted that we have considered the case of equal probability for the crack orientation. A certain order of the crack orientation may enhance our estimate of the mean noise level. Likewise, due to fluctuations the noise magnitude is rather large compared to the mean value $|\overline{\delta \mathbf{B}_t}|$.

The ULF magnetic noise occasionally observed prior to the strong crust earthquakes (e.g., see Fraser-Smith et al., 1990; Kopytenko et al., 1990; Hayakawa et al., 1996, 2000) lies in the frequency range of 0.01–1 Hz. The average level $|\overline{\delta \mathbf{B}_t}|$ related to square root of these characteristic frequencies gives the value of about 0.3–3 pT/Hz$^{1/2}$ that can serve as a rough estimate of the power spectrum magnitude. This assessment is consistent in magnitude with observation considering the uncertainties in the parameters. Moreover, it is worth mentioning that the seismic activity before and after earthquake occurrence may greatly enhance, which leads to increase of the actual value of regional seismicity parameter, $\dot{\beta}$, and eventually to increase of the ULF electromagnetic noise level.

In this paper we have dealt with alone tension cracks since the consideration of the shear cracks leads to very complicated expressions. Actually, all types of cracks including the tension and shear cracks are formed during rock fracture and probably the majority will tend to be shear ones (Scholz, 1990). If the shear cracks are predominant, the calculation technique developed above can be also applied. In contrast to the tension crack the shear one can radiate the seismic waves in such a way that the effective magnetic moment induced in the conductive medium is non-parallel to the vector $\mathbf{B}_0$ depending on the crack orientation (Surkov, 2001). As there is an equal probability for the shear crack orientation, the mean magnetic moment of the crack ensemble becomes zero. At the same time one may expect that the shear cracks will predominantly grow along the axis of maximal shear stresses or, more precisely, along the directions that make the angle 0.5 arctan k_{f} with this axis (Scholz, 1990). Here k_{f} denotes the coefficient of internal friction of the rock. Likewise, most of the shear cracks possibly will tend to be parallel to fault plane. Taken together, this means that the mean magnetic moment of the shear crack ensemble is non-zero. On account of the fact that the displacement jump, $[u_{\mathrm{s}}]$, along the shear crack surface is proportional to the crack length we come to an estimate similar to that given by Eq. (42). To summarize, we note that each crack species is capable to sustain generation of the ULF magnetic noise that can be detected by ground magnetometers.

Finally we arrive at the following conclusions.

1. It was shown that the rock fracture and energization of crack growth in conductive medium is accompanied by the ULF geomagnetic perturbations. If the crack-generated temporal series of acoustic impulses is a Poisson random process, the mean level of the electromagnetic noise is defined by the time integral of the magnetic field produced by a single crack. We have estimated this integral and thereby generalized the results of previous works.
2. It follows from our calculations that the large cracks make a main contribution to the ULF magnetic noise. The small cracks appear to have no effect due to strong damping of their signals. Inside the region where the acoustic damping is of minor importance the magnitude of the electromagnetic perturbations is found to decrease with distance as r^{-1}, while far from this region the mean level of the noise falls off more rapidly with distance, that is as r^{-3}. According to our estimations the magnitude of the electromagnetic noise can amount to the value which is greater than or of the order of 1 pT/Hz$^{1/2}$.
3. In the case of tension cracks the effect treated here can arise independently of the distribution of the crack plane orientation since the mean effective magnetic moment of the cracks always points in opposition to the geomagnetic field. In order to obtain the same effect, as the shear crack ensemble is considered, a certain order of the crack orientation is necessary. For example, the predominant directions for the shear crack growth can concentrate around the axis of maximal shear stresses.

Acknowledgements

This research was supported by ISTC under Research Grants No. 1121 and 2990.

References

Aki, K., Richards, P., 2002. Quantitative Seismology, second ed. Univ. Sci. Books, Sausalito, California, pp. 932.

Bernard, P., 1992. Plausibility of long electrotelluric precursors to earthquakes. J. Geophys. Res. 97B, 17531–17546.

Fenoglio, M.A., Johnston, M.J.S., Byerlee, J.D., 1995. Magnetic and electric fields associated with changes in high pore pressure in fault zones: application to the Loma Prieta ULF emissions. J. Geophys. Res. 100B, 12951–12958.

Fraser-Smith, A.C., Bernardi, A., McGill, P.R., Ladd, M.E., Helliwell, R.A., Villard Jr., O.G., 1990. Low-frequency magnetic field measurements near the epicenter of the Ms 7.1 Loma Prieta earthquake. Geophys. Res. Lett. 17, 1465–1468.

Freund, F., 2002. Seismic electric signals (SES) and the conductivity structure of the crust. In: Hayakawa, M., Molchanov, O. (Eds.), Seismo Electromagnetics: Lithosphere–Atmosphere–Ionosphere Coupling. TERRAPUB, Tokyo, pp. 141–152.

Gorbatikov, A.V., Molchanov, O.A., Hayakawa, M., Uyeda, S., Hattori, K., Nagao, T., Tanaka, H., Nikolaev, A.V., Maltsev, P., 2002. Acoustic emission possibly related to earthquakes, observed at Matsushiro, Japan and its implications. In: Hayakawa, M., Molchanov, O. (Eds.), Seismo Electromagnetics: Lithosphere–Atmosphere–Ionosphere Coupling. TERRAPUB, Tokyo, pp. 1–10.

Gutenberg, B., Richter, C.F., 1954. Seismicity of the Earth and Associated Phenomenon, second ed. Princeton University Press, Princeton.

Hayakawa, M., Hattori, K., 2004. ULF electromagnetics emissions associated with earthquakes: Review, Trans. Fundamentals and Materials, Special Issue on Electromagnetic Theory and Its Application, 124, 1101–1108.

Hayakawa, M., Kawate, R., Molchanov, O.A., Yumoto, K., 1996. Results of ULF magnetic field measurements during the Guam earthquake of 8 August 1993. Geophys. Res. Lett. 23, 241–244.

Hayakawa, M., Itoh, T., Hattori, K., Yumoto, K., 2000. ULF electromagnetic precursors for an earthquake at Biak, Indonesia on February 17, 1996. Geophys. Res. Lett. 27, 1531–1534.

Kopytenko, Yu.A., Matiashvili, T.G., Voronov, P.M., Kopytenko, E.A., Molchanov, O.A., 1990. Detection of ULF emissions connected with the Spitak earthquake and its aftershock activity, based on geomagnetic pulsation data at Dusheti and Vardzia observations, Preprint of IZMIRAN, 1990 (in Russian).

Molchanov, O.A., Hayakawa, M., 1995. Generation of ULF electromagnetic emissions by microfracturing. Geophys. Res. Lett. 22, 3091–3094.

Molchanov, O.A., Hayakawa, M., 1998. On the generation mechanism of ULF seismogenic electromagnetic emissions. Phys. Earth Planet. Inter. 105, 201–210.

Molchanov, O., Kulchitsky, A., Hayakawa, M., 2002. ULF emission due to inductive seismo-electromagnetic effect. In: Hayakawa, M., Molchanov, O. (Eds.), Seismo Electromagnetics: Lithosphere–Atmosphere–Ionosphere Coupling. TERRAPUB, Tokyo, pp. 153–162.

Rytov, S.M., 1966. Introduction to Statistic Radiophysics. Fizmatgiz, Moscow (in Russian).

Scholz, C.H., 1990. The Mechanics of Earthquakes and Faulting. Cambridge Univ. Press.

Slifkin, L., 1993. Seismic electric signals from displacement of charged dislocations. Tectonophysics 224, 149–152.

Surkov, V.V., 1997. The nature of electromagnetic forerunners of earthquakes, Transactions (Doklady) of the Russian Academy of Sciences. Earth Sci. Sections 355, 945–947.

Surkov, V.V., 1999. ULF electromagnetic perturbations resulting from the fracture and dilatancy in the earthquake preparation zone. In: Hayakawa, M. (Ed.), Atmospheric and Ionospheric Phenomena Associated with Earthquakes. TERRAPUB, Tokyo, pp. 357–370.

Surkov, V.V., 2000. Electromagnetic Effects Caused by Earthquakes and Explosions. MEPhI press, Moscow (in Russian).

Surkov, V.V., 2001. The role of shear cracks in the formation of electromagnetic noise preceding some earthquakes. Doklady Earth Sci. 377A, 349–355 (Translated from Doklady Akademii Nauk. Russian Academy of Science).

Surkov, V.V., Tanaka, H., 2005. Electrokinetic effect in fractal pore media as seismoelectric phenomena, In: Fractal Behaviours of the Earth System, V.P. Dimri (Ed.), 83–96, Springer-Verlag, Berlin, Heidelberg, New York, in press.

Surkov, V.V., Uyeda, S., Tanaka, H., Hayakawa, M., 2002. Fractal properties of medium and seismoelectric phenomena. J. Geodynamics 33, 477–487.

Surkov, V.V., Molchanov, O.A., Hayakawa, M., 2003. Pre-earthquake ULF electromagnetic perturbations as a result of inductive seismomagnetic phenomena during microfracturing. J. Atmos. Solar–Terr. Phys. 65, 31–46.

Turcotte, D.L., 1997. Fractal and Chaos in Geology and Geophysics, second ed. Cambridge University Press.

Varotsos, P., Alexopoulos, K., 1984a. Physical properties of the variations of the electric field of the earth preceding earthquake, I. Tectonophysics 110, 73–98.

Varotsos, P., Alexopoulos, K., 1984b. Physical properties of the variations of the electric field of the earth preceding earthquake. II. Determination of epicenter and magnitude. Tectonophysics 110, 99–125.

Varotsos, P., Alexopoulos, K., 1986. Stimulated current emission in the earth: piezostimulated currents and related geophysical aspects. In: Amelinckx, S., Gevers, R., Nihoul, J. (Eds.), Thermodynamics of Point Defects and their Relation with Bulk Properties. North Holland, Amsterdam, pp. 136–142, 403–406, 410–412, 417–420.

Varotsos, P.A., Sarlis, N.V., Skordas, E.S., 2002. Long-range correlations in the electric signals that precede rupture. Phys. Rev. 66E. doi:10.1103/PhysRevE.66.011902.

Varotsos, P.A., Sarlis, N.V., Skordas, E.S., 2003. Long-range correlations in the electric signals that precede rupture: Further investigations. Phys. Rev. 67E. doi:10.1103/PhysRevE.67.021109.